Journal of Information Engineering and Applications
ISSN 2224-5782 (print) ISSN 2225-0506 (online)
Vol.3, No.7, 2013

A High Performance Model for Rainfall Effect on Radio Signals

Jonathan U. Agber Johnson Mise Akura
Department of Electrical and Electronics Engineering
Federal University of Agriculture, Makurdi, Benue State, Nigeria.
*E-mail: juagber@gmail.com Email: akuramise@yahoo.com

Abstract
A mathematical model for calculating the attenuation due to rain is derived using spheroid rain drops over a broad frequency range. The model is based on the limitation of Okumura's model which does not account for other forms of losses, like rainfall, haze, etc. Numerical results are obtained from the simulation of the free space model and the formulated model with drop size of 3.5mm over a broad frequency range of 3GHz, 5GHz and 10 GHz using MATLAB software package. The validity of the formula for computing rain attenuation is then checked by comparing the results of the simulation of the path loss and received power as function of distance between the separations of two antennas with that of the free space model. The results obtained show that the attenuation (path loss) due to rainfall is 75.46% greater than that due to free space; and the received power for the rainfall model is 24.61% less than that due to the free space model.
Keywords: Radio communication, Radio wave interference, Rainfall model, Rainfall losses, Rainfall attenuation

1. Introduction

The medium through which radio waves traverse places some basic limitations on the performance of wireless telecommunication systems. This has a very big role to play in wireless communication systems; it is the main contributor to many impairments of wireless systems performance. The huge impairments make wireless communication unpredictable and offer random analysis. Rain attenuation is caused by the scattering and absorption of electromagnetic waves by drops of liquid water. The scattering diffuses the signal, while absorption involves the resonance of the waves with individual molecules of water. Absorption increases the molecular energy corresponding to a slight increase in temperature, and results in an equivalent loss of signal energy. The study of radio waves scattering and absorption by raindrops therefore becomes very important since rain attenuation data due to radio waves scattering and absorption are needed in many important applications, including microwave propagation systems, remote sensing systems, radar systems, and radio link systems [1]. From the view point of radio communication network engineering, communication medium can be viewed as imperfect bit pipes; the imperfection being that the bit pipes can delay, loose or modify the information they carry [2]. Rain attenuation is affected by factors such as rain rate, operating frequency, the physical size of drops and polarization [1], [3]. During a period of heavy rainfall, raindrops fall with a significant canting angle because of the strong winds usually associated with such events. Hence, rain attenuation is related to the rain rate and the scattering and absorption mechanism of raindrops at the operating frequency [4]. Although studies of rain attenuation of microwave signals have been conducted in Europe and the United States dating back to the 1940s, it is now common knowledge that the rain-attenuation models and raindrop size distribution models are highly regionalized[5], [6]. So many people have worked on rain rates and rain attenuation models: Calla et.al [7] worked on the effect of rain and dust on propagation of radio waves within millimeter wavelength. In their experiment, they placed rain gauge, and dust particle near the receiver to avoid shadowing effect due to nearby objects. The specification of the LOS link can also be used for the horizontal path attenuation. The vertical path attenuation was then estimated by subtracting clear sky attenuation (free space) from excess attenuation (rainy medium) due to rain. Henry researched on rain induced bistatic scattering at 60 GHz. In their work, they operated at 94 GHz as proposed by Gloaguen and Lavergnat. The first order multiple scattering approximation is applicable to the scattering at 60 GHz. Hence they used the bistatic radar equation [8] for the particle scattering by rain. Ojo et.al. [9] worked on rain rate and rain attenuation prediction for satellite communication in Ku and Ka bands over Nigeria. They used a model that was developed by Moupfouma and Martins to predict rain rate and concluded that the model is good for tropical and temperate climate [10]. The map for the rain attenuation over Nigeria was developed using the ITU rain attenuation [11]. The results obtained from their research confirm that 0.1% of time of rain attenuation is needed for very small aperture terminal (VSAT) network service availability. Capsoni et.al. [12] researched on the multiple excel model for the prediction of the radio interference due to hydrometeor scattering. They used a physically-based method for the prediction of the radio interference due to hydrometeor scattering. The coupling-by-scattering mechanism relies on the bistatic radar equation which allows for evaluation of interference levels when the electrical and geometrical characteristics as well as the distribution of scatterers in the common volume are known. Hence, they used the bistatic radar equation (BRE) to solve for a population of isolated exponential rain cells (EXCELL) model which generates complex synthetic rain fields reflecting the total first and second order features of the rainfall process. Saikia et

al [13] worked on rain attenuation of centimeter radio waves in which they used the laser disnometer for calibrating and profiling of rain drop size distribution. The rain drop signature is extracted by allowing the drops to pass through a controlled field of view of a sensor. The laser beam was used as the signal source, the phototransistor was used as detector-cum-amplifier and optical fibres as trans-receiving ports. Rain drops size and rain rate at different weather condition were measured. The specific attenuation of the line of sight radio signals at 10-30 GHz of various drop diameters were then calculated using standard attenuation equations and model values of scattering function.

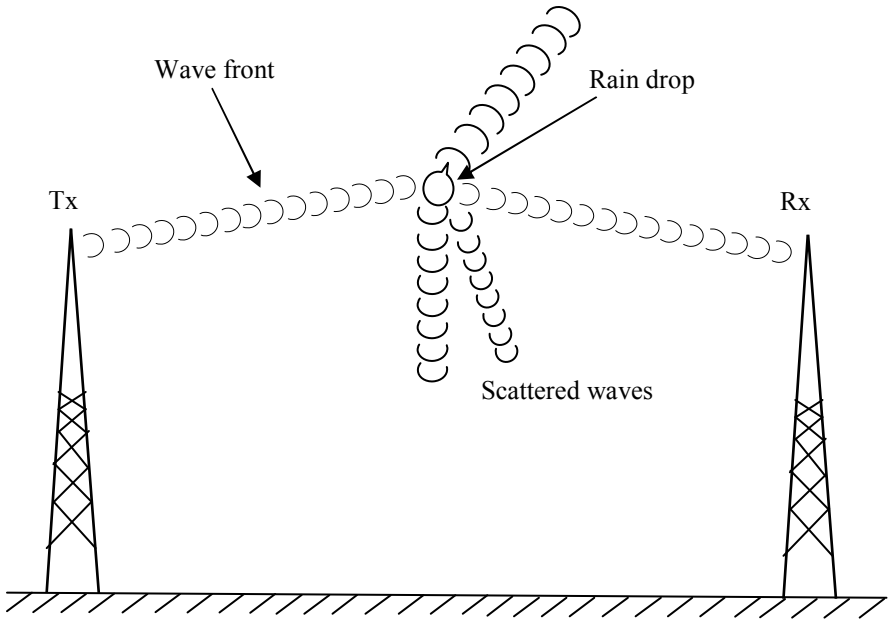

Figure 1: Interference of Signals by Rain Drop

2. Development of the model

Radio signals are transmitted from Tx, and when they encounter drops of rain, the waves are scattered in diverse directions and others are absorbed by the rain drops; which acts as poor dielectric, absorbing power from the radio waves and dissipating the power by heat loss. This is shown in Figure 1.

In deriving an expression for the attenuation of electromagnetic waves traversing through rain, consideration is given to a volume, which is bounded by a cone of the power flux lines and two spherical surfaces as shown in Figure 2. P_i corresponds to the component of power emitted from the transmitter, Tx, which is the source power. Part of the power is absorbed in the volume while the other part is scattered by the different components in the volume. Those components of the power that are neither scattered nor absorbed in the volume are refracted and they reach the receiver, Rx [14].

If P_{sc} represents the power that is scattered by the component of rain drops in the volume, while P_{ab} represents the component of power that is absorbed by rain drops in the volume, and P_r represents the component of power that is refracted (transmitted signals that reach the receiver), then, the power balance in the beam is given by [15] as:

$$P_i = P_{sc} + P_{ab} + P_r \quad (1)$$

This equation is feasible because, the incident power P_i radiated from the source power is split into various components of power as the waves come in contact with a drop of rain [14]. Each of the power components can

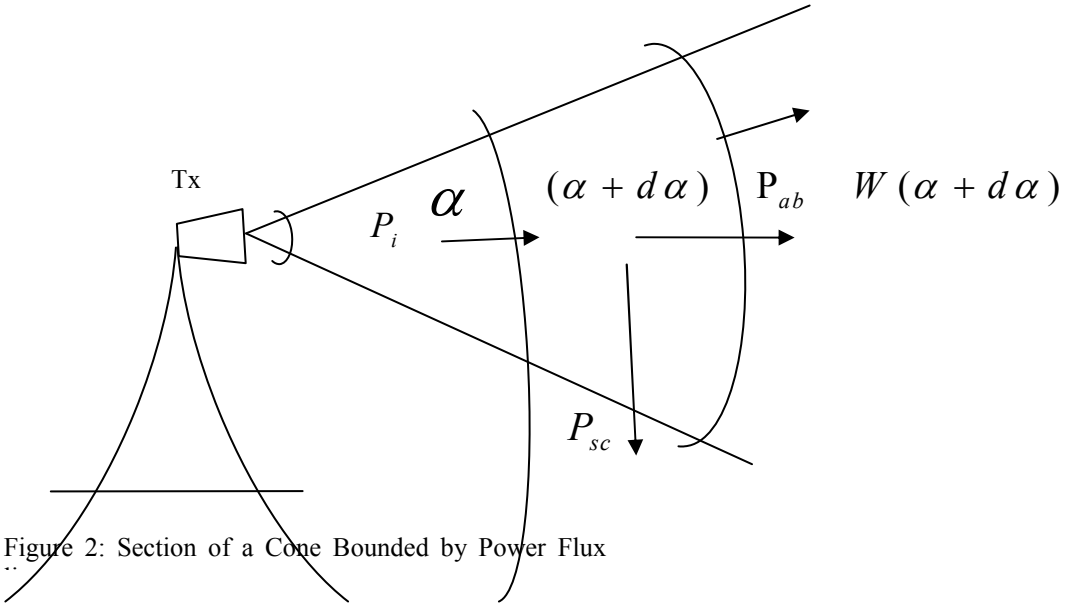

Figure 2: Section of a Cone Bounded by Power Flux

therefore be expressed in terms of the time-average Poynting vector which is given by [16] as:

$$W_{av}(\alpha) = \{W(\alpha, t)\} = \frac{1}{2} R_e \{E(\alpha, t) \times H^*(\alpha, t)\} \quad (2)$$

where: $W(\alpha, t)$ is the power density as function of distance and time,

$E(\alpha, t)$ is the electric field,

$H^*(\alpha, t)$ is the magnetic field strength,

α is the distance between the two antennas.

The equation of the time-average Poynting vector gives the value of the power density $\left(w/m^2\right)$. Hence each component of the power can be easily evaluated in terms of the time-average value of the Poynting vector, such that

$$P_i = W_{av}(\alpha) \, n \, \alpha^2 d\Omega \quad (3)$$

where *n* is the normal of the first surface,

$d\Omega$ is the differential solid angle which is defined as $d\Omega = \sin\theta d\phi$,

$\alpha^2 d\Omega$ is the spherical surface area,

θ is the elevation or altitude,

ϕ is the azimuth – angular measurement in a spherical coordinate system.

As the symmetry is spherical, the projection of the average power density is the same as the average power density [13]. Thus,

$$W_{av}(\alpha) = W_{av} n \quad (4)$$

Each component of power can, therefore, be expressed in terms of the time-average Poynting vector [17]. To obtain the various components of power discussed earlier on, consideration is given to the drop size distribution denoted as $N(d)$, the scattering cross section and absorption cross section in the volume in which the signal is scattered or absorbed. The scattering cross section is the region within which the signal is scattered in the volume and is denoted as σ_{sc}, while the region or area within which the signal is absorbed by the rain drop in the volume is denoted as σ_{ab}. Hence the total cross section of scattering and absorption of the signal in the volume is the sum of the scattering cross section and absorbing cross section and is given by [14] as:

$$\sigma_{total} = \sigma_{sc} + \sigma_{ab} \quad (5)$$

This leads to the assumption that the total power loss is due to scattering and absorption [14]. The power loss due to scattering can be obtained by multiplying the average power density, $W(\alpha)$, the volume in which the signal is scattered, V, the drop size distribution, $N(d)$, and the scattering cross section σ_{sc} [14]. Hence

$$\left.\begin{array}{l} P_{sc} = W(a)V\,N(d)\sigma_{sc} \\ Similarly, \\ P_{ab} = W(a)V\,N(d)\sigma_{ab} \end{array}\right\} \quad (6)$$

The volume V can therefore be approximated by $\alpha^2 d\alpha d\Omega$; that is multiplying the surface area by the solid angle [17], then

$$\left.\begin{array}{l} P_{sc} = W(a)\alpha^2 d\alpha\, d\Omega\, N(d)\sigma_{sc} \\ and \\ P_{ab} = W(a)\alpha^2 d\alpha\, d\Omega\, N(d)\sigma_{ab} \end{array}\right\} \quad (7)$$

The refracted power is given in equation (8) as:

$$P_r = W(\alpha)(\alpha + d\alpha)(\alpha + d\alpha)^2 \Omega \quad (8)$$

Hence equation (1) becomes:

$$dW(\alpha)\alpha^2 d\Omega = W(\alpha)\alpha^2 d\alpha\, d\Omega N(d)\sigma_{sc} + W(\alpha)\alpha^2 d\alpha\, d\Omega N(d)\sigma_{ab} + W(\alpha)(\alpha + d\alpha)(\alpha + d\alpha)^2 \Omega$$

which is then simplified to yield equation (9)

$$\frac{W(\alpha)(\alpha + d\alpha)(\alpha + d\alpha)^2 + \alpha^2 W(\alpha)}{d\alpha} + \alpha^2 W(\alpha) N(d)\sigma_{total} = 0 \quad (9)$$

Hence, $(\alpha + d\alpha)^2$ from equation (9) can be further simplified by applying Taylor's series expansion, in which the equation will reduce to:

$$(\alpha + d\alpha)^2 = \alpha^2\left(1 + \frac{d\alpha}{\alpha}\right)^2 = \alpha^2\left(1 + 2\frac{d\alpha}{\alpha}\right) = \alpha^2 + d\alpha, \quad for \ \frac{d\alpha}{\alpha} << 1$$

Hence

$$\frac{W(\alpha)(\alpha + d\alpha)(\alpha + d\alpha)^2 + \alpha^2 W}{d\alpha} + 2W(\alpha)(\alpha + \mathrm{d}\alpha) + \alpha^2 W N(d)\sigma_{total} = 0, \quad d\alpha \to 0$$

As $d\alpha \to 0$, the differential equation for the transmitted power density becomes:

$$\frac{dW(\alpha)}{d\alpha}\alpha^3 + N(d)W(\alpha)\alpha^2\sigma_{total} + 2\alpha W(\alpha) = 0 \quad (10)$$

Equation (10) has the general solution of second-order differential equation

$$W(\alpha) = \frac{c\, e^{-[N(d)\sigma_{total}]\alpha}}{\alpha^2}, \quad \alpha \neq 0 \quad (11)$$

where *c* is an arbitrary constant which can be evaluated by considering the power density, $W_{iso}(a)$ emitted in a spherical wave beam generated by an isotropic antenna with a time-average radiated power, P_s, (source power) [17]. The equation of the emitted power density in a spherical wave beam generated by an isotropic antenna is given in equation (12), as:

$$W_{iso}(\alpha) = \frac{P_s}{4\pi\alpha^2} \quad (12)$$

If equation (11) is compared with equation (12), which is the case for signals propagating in free space, i.e., $N(d)\sigma_{total}\alpha = 0$ then the constant *c* can be found as follows:

$$W_{iso}(\alpha) = \frac{P_s}{4\pi\alpha^2} = W_{av}(a) = \frac{c}{\alpha^2}, \ \alpha \neq 0$$

which gives $c = \frac{P_s}{4\pi}$

and thus reducing equation (11) to

$$W(a) = \frac{P_s e^{-[N(d)\sigma_{total}]\alpha}}{4\pi\alpha^2}, \quad \alpha \neq 0 \tag{13}$$

However, an isotropic antenna is not realizable in practice and is useful only for comparison purposes. A more practical type is the directional antenna which radiates more power in some directions and less in other directions [15]. The commonly used parameter to measure the overall ability of an antenna to direct radiated power in a given direction is a dimensionless quantity called the directive gain. The directive gain is defined in terms of the radiation intensity, $I(\theta,\phi)$, which is the time-average power per unit solid angle. Since there are α^2 square meters for each unit solid angle, radiation intensity $I(\theta,\phi)$ equals α^2 multiplied by the magnitude of the time-average Poynting vector, W_{av} [18].

Therefore,

$$I(\theta,\phi) = \alpha^2 W_{av}(\alpha,\theta,\phi) \tag{14}$$

The total radiated time–average power is related with the radiation intensity given by Lin and Chen [18] as:

$$P_s = \oint I(\theta,\phi)d\Omega \tag{15}$$

Since the antenna has the ability to direct radiated power in a given direction, the directive gain of the antenna also has a major role to play in the quality and quantity of the signals obtained by the receiver. The directive gain $G_d(\theta,\phi)$ of an antenna pattern is the ratio of the radiation intensity $\mathrm{I}(\theta,\phi)$ in the direction to the time-average radiated power [18]:

$$\mathrm{G}_d(\theta,\phi) = \frac{I(\theta,\phi)}{P_s / 4\pi} \tag{16}$$

Since the radiation from the antenna is not uniformly distributed, the expression of the attenuated time–average power density equation (13) has to be improved to include this property. Substituting equation (14) into equation (16) yields

$$W_{av}(a) = \frac{P_s e^{-[N(d)\sigma_{total}]\alpha}}{4\pi\alpha^2} G_d(\theta,\phi), \quad \alpha \neq 0 \tag{17}$$

If a receiving antenna is used to measure the transmitted power P_t at a distance a from the transmitter, that is the power that is neither absorbed nor scattered in the volume, the properties of the receiving antenna have to be considered [19]. The incident waves are being received in an area that is small compared to the physical area of the receiving antenna. This is the effective area, $\mathrm{A}_e(\theta,\phi)$ of the antenna and is defined as the ratio of the average power P_L delivered to a matched load to the time–average power density of the incident wave [19]. Hence,

$$\mathrm{P}_L = \mathrm{W}\,\mathrm{A}_e(\theta,\phi)$$

P_L is the maximum average power transferred to the load when the receiving antenna is oriented with the polarization of the incident wave [19]. The ratio of the directive gain and effective area of an antenna is a universal constant [19] and;

$$G_d(\theta,\phi) = G_r(\theta,\phi) = \frac{4}{\lambda^2} A_e(\theta,\phi) \tag{18}$$

where λ is the wavelength of the radio signal.

An expression for the received power P_R can therefore be obtained by multiplying the receiving antenna effective area $A_e(\theta,\phi)$ with the expression for the transmitted time-average power density $G_t(\theta,\phi)$ [17].

$$P_R = \frac{P_s e^{-[N(d)\sigma_{total}]\alpha}}{4\pi\alpha^2} G_t(\theta,\phi)\,\mathrm{A}_e(\theta,\phi) \tag{19}$$

Substituting equation (18) into equation (19) for $A_e(\theta,\phi)$ gives

$$P_R = \frac{P_s \lambda^2}{4\pi\alpha^2} G_t\,\mathrm{G}_r\,\mathrm{e}^{-[N(d)\sigma_{total}]\alpha} \tag{20}$$

where G_r is the receiver gain.

Table 1: The simulated results of the path loss for the rainfall attenuation model (RAM) and free space model

Separation between two antennas (Km)	**Data due to the effect of rainfall**			**Data due to the effect of free space**		
	3Ghz	4GHz	10GHz	3Ghz	4GHz	10GHz
1	469	475	493	97.1	103	121
2	483	489	507	111	117	135
3	491	497	515	119	125	143
4	497	502	521	125	131	149
5	501	507	525	129	135	153
6	505	511	529	133	139	157
7	508	514	532	136	142	160
8	511	516	535	139	144	163
9	513	519	537	141	147	165
10	515	521	539	143	149	167
11	517	523	541	145	151	169
12	519	524	543	147	153	171
13	520	526	544	148	154	172
14	522	527	546	150	156	174
15	523	529	547	151	157	175
16	524	530	548	153	158	177
17	526	531	550	154	159	178
18	527	532	551	155	161	179
19	528	534	552	156	162	180
20	529	535	553	157	163	181
21	530	536	554	158	164	182
22	531	537	555	1.59	165	183
23	532	537	556	160	166	184
24	532	538	557	161	166	185
25	533	539	557	161	167	186
26	534	540	558	162	168	186
27	535	541	559	163	169	187
28	536	541	560	164	169	188
29	536	542	560	164	170	188
30	537	543	561	165	171	189

Two antennas can be aligned in such a way that they have maximum value of the directive gain for effective radio communication. Hence, the maximum directive gain of an antenna can be represented by the directivity of the antenna [14]. Thus, if the directivity of the transmit antenna is represented by D_t and that of the receive antenna represented by D_r, equation (19) can be restated as:

$$\frac{P_R}{P_s} = \frac{\lambda^2 D_t D_r}{4\pi\,\alpha^2} \mathrm{e}^{-[N(d)\sigma_{total}]\alpha} \tag{21}$$

The path loss denoted as L can be evaluated by finding the reciprocal of equation (20), given as;

$$L = \frac{P_s}{P_R} = 10\log\frac{4\pi\alpha^2}{\lambda^2 D_t D_r} \mathrm{e}^{[N(d)\sigma_{total}]\alpha} \tag{22}$$

Table 2: The simulated results of the received power for the rainfall attenuation model (RAM) and free space model

Separation between two antennas (Km)	Data due to the effect of rainfall			Data due to the effect of free space		
	3Ghz	4GHz	10GHz	3Ghz	4GHz	10GHz
1	213	211	203	1030	973	825
2	207	205	197	901	857	741
3	204	201	194	840	801	699
4	201	199	192	801	766	672
5	200	197	190	774	741	652
6	198	196	189	752	721	637
7	197	195	188	735	705	625
8	196	194	187	721	692	614
9	195	193	186	709	681	606
10	194	192	186	699	672	598
11	193	191	185	690	663	591
12	193	191	184	681	656	585
13	192	190	184	674	649	580
14	192	190	183	667	643	575
15	192	189	183	661	637	570
16	191	189	182	656	632	566
17	190	188	182	650	627	562
18	190	188	182	646	623	559
19	189	187	181	641	618	555
20	189	187	181	637	614	552
21	189	187	181	633	611	549
22	188	186	180	629	607	547
23	188	186	180	626	604	544
24	188	186	180	623	601	541
25	188	186	179	619	598	539
26	187	185	179	616	595	537
27	187	185	179	614	593	535
28	187	185	179	611	590	532
29	186	184	178	608	588	531
30	186	184	178	606	585	529

3. Validation of the model

The formula for the rain attenuation developed using incident electromagnetic waves for oblate spheroidal raindrops with mean (effective) drop radius ranging up to 0.35 cm and frequencies of 3GHz to 10 GHz; is compared with free space model of the Okumura- Hata free space model.

The formulated rainfall model and the free space model are simulated using MATLAB software package and data obtained from the simulation and the results are tabulated in Tables 1 and 2. From the simulation, the received power and the path loss in both cases are plotted against the distance between the separation of the transmit and receive antennas and the result is compared and summarized as shown in Figures 3, 4, 5 and 6.

Table 2: The simulated results of the received power for the rainfall attenuation model (RAM) and free space model

4. Analysis of results

4.1 Path loss as a function of distance for the rain attenuation and free space models for signals of 3, 4, and 10 GHz

Path loss is an important parameter which must be taken into consideration when planning for a radio communication system [19]; this helps to determine the distance at which one antenna will be sited from the other. The parameter is also important in determining the hand off speed and cell sizes [20]. The simulation results, shown graphically in Figures 3 and 4, are for path loss plotted against the distance between the separations of the two antennas for the rain attenuation model and free space model. From the graphs, the output result of the rain attenuation model is higher compared to the output result of the free space propagation model for all the three frequencies. This accounts for the fact that, degradation of the radio signals occurs as the waves

traverse through rain. It is also easy to see that the two curves rise exponentially as the separation between the antenna increases; this could be as a result of the fact that the attenuation produced increases exponentially as the signal decays gradually.

Though, there is exponential rise in the two curves in the same manner, there is a relatively higher path loss in the rain attenuation model than the free space model, thus confirming the result obtained by Head, [21].The analysis of the behavior of the graph at 10GHz is not different from that at 3GHz and 4GHz. From the graph, the level of attenuation of the radio signal at 10GHz is higher compared to the other operating frequencies [22, 23]. Thus, one can conclude that as the operating frequencies increase, there is higher level of attenuation of the signals. Also, an increase in the separation between the two antennas results in higher path loss.

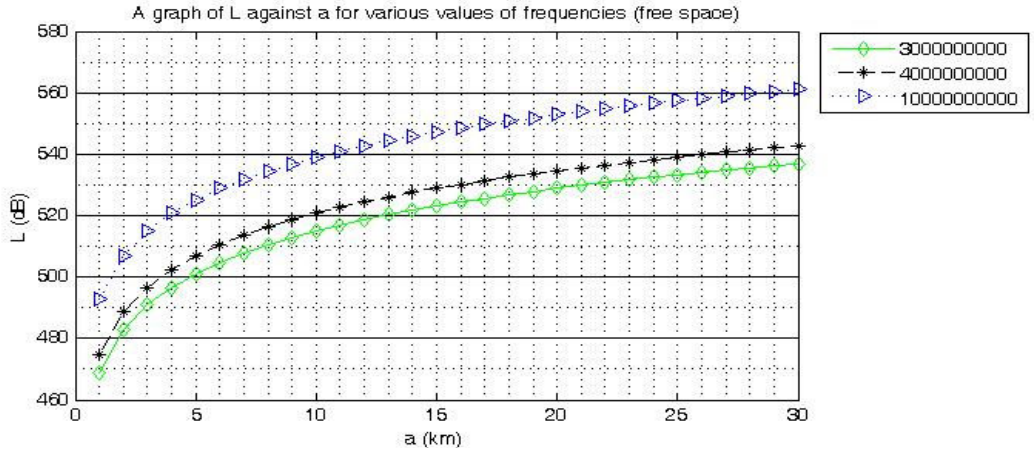

Figure 3: The Graph of the Rain Attenuation Path Loss Model Against the Separation Between the Two Antenna

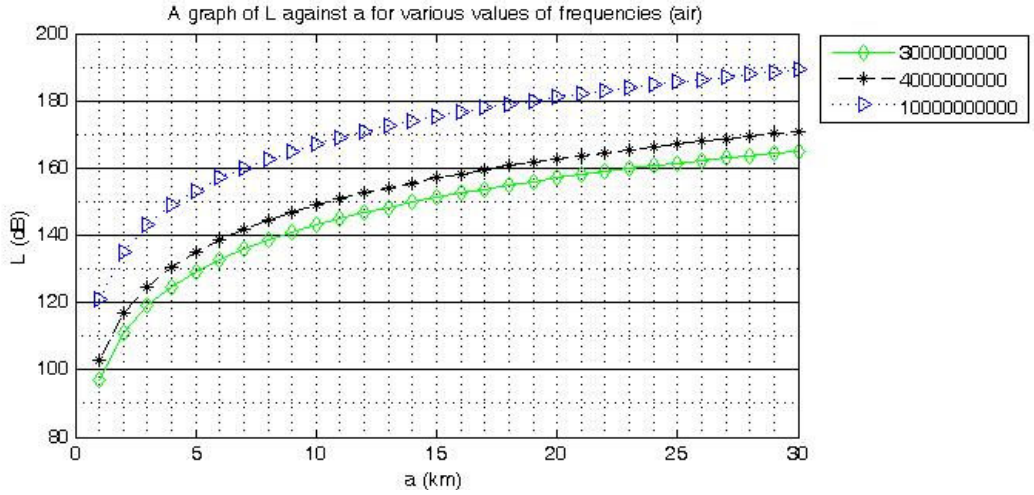

Figure 4: The Graph of the Free Space Path Loss Against the Separation Between the Two Antenna

4.2 Received power as a function of distance for the rain attenuation and free space models for signals of 3, 4, and 10 GHz

The received power is a parameter that is very significant in communication; this parameter was also obtained during simulation and plotted in Figures 5 and 6. The signal strength at the receive antenna determines the amount of power that is satisfactorily required to obtain coverage in an area. It was observed from Figures 4 and 5 that the output results at various frequencies for both models slope down gradually; with the graphs representing the output results for the free space higher than that due to the effect of rain.

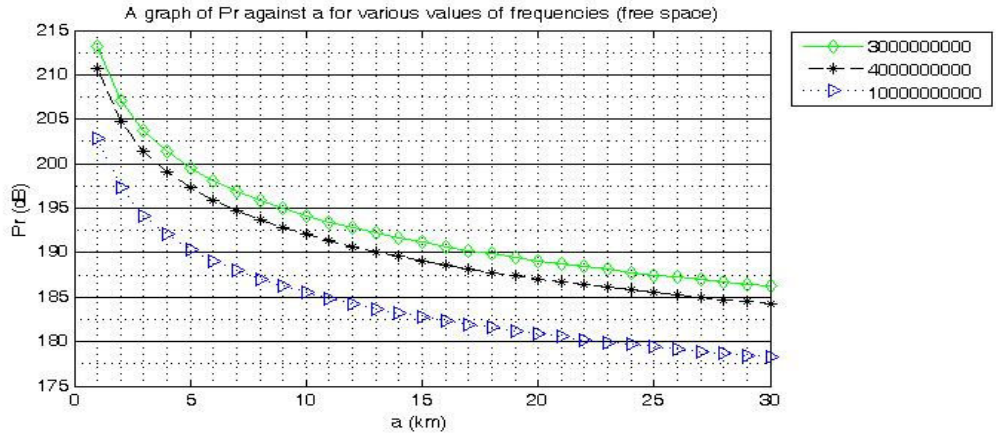

Figure 5: The Graph of the Received Power Against the Separation Between the Two Antennas for the Rainfall Model

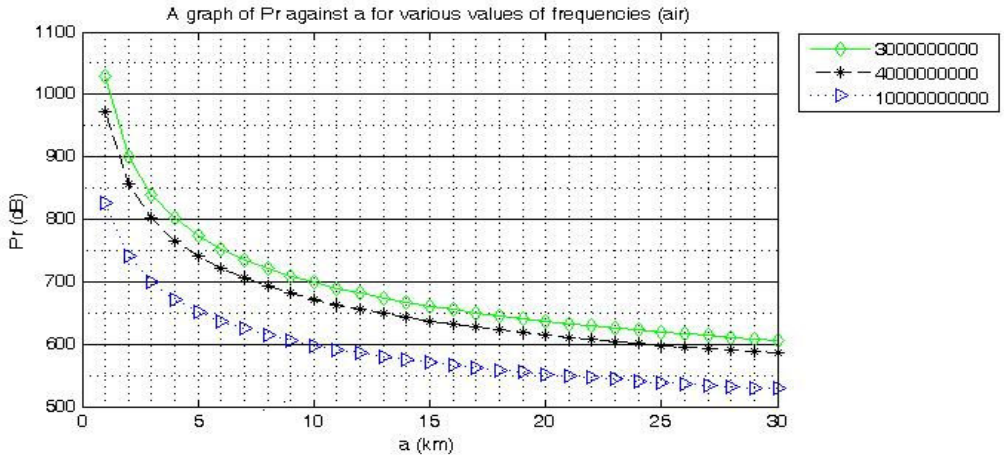

Figure 6: The Graph of the Received Power Against the Separation Between the Two Antennas for the Free Space Propagation Model (FSPM)

The behavior of the graphs is because, as the attenuation (path loss) increases with increase in distance, the received power decreases as the distance between the receive and transmit antennas increases. A similar observation was made by Gilbert, [24]. It was also observed that the received power is higher in the free space since the signal at all frequencies traverses under a clear line of sight, while that due to the effect of rain is absorbed by drops of rain or scattered in diverse directions therefore, has higher attenuation and less received power [20]

5. Conclusions

The equation for the path loss, equation (22), derived here is useful for the calculation of specific microwave attenuation due to raindrops in the frequency range from 0.6 to 100 GHz. It provides a simple method for quickly calculating the microwave rain attenuation as a function of frequency, the separation between two antennas and mean radii of raindrops. This formula thus provides a simple and inexpensive method for calculating attenuation caused by raindrops as they are propagated, which otherwise requires complicated, tedious, and expensive algorithms. By inputting the parameters, as used in the formula, a new numerical method for the calculation of specific rain attenuation is established. The validity of the formula for calculating the specific rain attenuation is then checked by comparing the obtained results of specific rain attenuation with those obtained by free space model.

The calculation of microwave rain attenuation can now be carried out for a wide range of frequencies and rain rates. This formula of specific rain attenuation makes it practical for direct use by wireless communication system designers. From the studies, it was observed that when the specific rain attenuation is predicted in different areas, it is important to take into account the effects of drop-size and the operating frequencies.

References

1. Murat Uysal, (2001). *Cooperative Communication for Improved Wireless Network Transmission, Framework of Virtual Antennas.* University of Waterloo, Canada.
2. Longley-Rice, A. G. (1999). Prediction of Tropospheric Radio Transmission Loss Over Irregular Terrain: A Computer Method**,** *Institute of Telecommunication Science, ESSA Tech. Rep* ER 100-ITS 02, Boulder. Co.
3. Theodore S. Rappaport, (2000). *Wireless Communication, Principles and Practice*; 2^{nd} Edition. Pearson Education Inc. Singapore
4. Barber, P. and Yeh, C., (1975) "Scattering of electromagnetic waves by arbitrarily shaped dielectric bodies, *Journal of Meteor,* Vol. 14, pp. 2864-2872.
5. Rutherford Appleton Laboratory, (1990) Factors in Predicting Radiowave Attenuation Due to Rain. *Proc. URSI Commission F Open Symp. Region*
6. URSI Standing Committee on Developing Countries, (1996). *Handbook on Radio propagation Related to Satellite Communications in Tropical and Subtropical Countries*.
7. Calla, O. P. N. and Purohit, J .S. (1971) International Centre for Radio Science, 'OM NIWAS' A-23 Shastri Nagar Jodhpur 242003, pp1143-1159
8. Ishimaru, A. (1976) "*Wave Propagation and Scattering in Random Media*", IEEE Press and Oxford University Press, NY USA, pp 1232-1241
9. Ojo, J. S., Adewole, M. O. and Sarkar, S. K., (2008). Rain rate and Attenuation Prediction for Satellite Communication in Ku Ka Bands over Nigeria. *Progress in Electromagnetics Research.* B, Vol.5, pp. 207– 223
10. Moupfouma, F. and Martin, L. (1995), Modeling of Rain rate Cummulative Distribution for the Design of Satellite and Terrestrial Communication Systems, *Int. Journal of Satellite Communication* 13(2), pp 105-115
11. Crane, R. K. (1985). Evaluation of Global and CCIR Models for Estimation of Rain rate Statistics. *Radio Science,* 20(4), pp 865-879
12. Capsoni, C., Luini, L. and Amico, M. D. (1997). A Physically-base, Simple Prediction Method for Scattering Interferences. *Radio Science,* Vol.32, No.2, pp. 397-409
13. Saikia, M., Devi, M., Barbara, A. K. and Sarmar , H. K. (2009). Raindrop Size Distribution Profiling by Laser Disdrometer and Rain Attenuation of Centimeter Radio Waves. *Indian Journal of Radio Science and Space Physics,* Vol. 38, pp 80-85
14. Walsch, J. and Bertoni H. L., (1998). A Theoretical Model of UHF Propagation in Urban Environments. *IEEE Trans. Antennas and Propagation*. Vol. AP-36, pp 1788-1794.
15. Lin, D. P. and Chen H. Y. (2001). Volume Integral Equation Solution of Extinction Cross Section by Raindrops in the Range of 0.6-100GHz. *IEEE Trans. Antennas and Propagation.* Vol. 49, pp494-499
16. Tzler, C.M., (1994). Microwaves (1-100GHz) Dielectric Model of Raindrops. *IEEE Trans. Geoscience and Remote Sensing.* Vol. 32, No5, pp 947 – 949
17. Ulaby, F. and M. Rayes, (1987) Microwaves Dielectric Spectrum of Vegetation. Part II: Dual – dispersion Model. *IEEE Trans. Geoscience and Remote Sensing*. GE – 25(5), pp 550 – 556
18. Kirdyashav K. P., Chuckhlantsev A. A., and Sutko A. M., (1979). Microwave Radiation of the Earth Surface in the presence of Raindrops. *Radio science and Electronics.* Vol. 24, pp 256 – 264
19. Alisebrook, K. and Parsons, J. D. (1997). Mobile Radio Propagation in British Cities at Frequencies in the HF and UHF Bands. *IEEE Trans.* Vol 26, pp. 313 – 323.
20. Papazian, B. P., Hufford, G. A., Achatz, R. J. and Hoffman, J. R. (1997). Study of the Local Multipoint Distribution Service Radio Channel. *IEEE Trans. Broadcasting*. Vol 43 (2), pp. 175 – 184.
21. Head, H. T. (1999) The Influence of Rain on Television Field Strength at U – H Frequencies, *Proc IRE*. Vol. 48, pp 1016 – 1020.
22. Liolis, K, P., Panagopoulos, A. D. and Scalise, S. (2010). Combination of Tropospheric and Local Environment Effects for Mobile Satellite Systems above 10 GHz. *IEEE Trans. Veh. Technol.,* Vol. 59, No 3, pp. 1109 – 1120.
23. Head, H. T. (1999) The Influence of Rain on Television Field Strength at U – H Frequencies, *Proc IRE*. Vol. 48, pp 1016 – 1020.
24. Liolis, K, P., Panagopoulos, A. D. and Scalise, S. (2010). Combination of Tropospheric and Local Environment Effects for Mobile Satellite Systems above 10 GHz. *IEEE Trans. Veh. Technol.,* Vol. 59, No 3, pp. 1109 – 1120.
25. Gilbert, E.N. (1985). Energy Reception for Mobile Radio. *BSTJ.* 44, pp. 1779 – 1803.

Jonathan U. Agber received MSc degree in electromechanical Engineering from the Moscow Power Engineering Institute, Moscow, Russia in 1976, PhD degree in Electrical Engineering from the University of Newcastle Upon Tyne in the UK in 1985. He is a Senior Lecturer in the Department of Electrical and Electronics Engineering, The Federal University of Agriculture, Makurdi, Benue State, Nigeria. He is a registered engineer and Member Nigerian Society of Engineers. His research interest includes CAD, simulation and control of incremental motion devices and software development.

Johnson M. Akura is a lecturer with the Department of Electrical and Electronics Engineering, The Federal University of Agriculture, Makurdi, Benue State, Nigeria where he obtained B.Eng degree in 2006. He received his M.Eng at the University of Nigeria Nsukka in 2012. His research interest includes semiconductor devices and nano-technology.